Journal of Solid State Chemistry 183 (2010) 2305–2308

Contents lists available at ScienceDirect

Journal of Solid State Chemistry

journal homepage: www.elsevier.com/locate/jssc

Anisotropic compression of a synthetic potassium aluminogermanate zeolite with gismondine topology

Young-Nam Jang [a], Chi-Chang Kao [b], Thomas Vogt [c], Yongjae Lee [d,*]

[a] Korea Institute of Geoscience and Mineral Resources, Daejeon 305-350, Republic of Korea
[b] National Synchrotron Light Source, Brookhaven National Laboratory, Upton, NY 11973, USA
[c] NanoCenter & Department of Chemistry and Biochemistry, University of South Carolina, Columbia, SC 29208, USA
[d] Department of Earth System Sciences, Yonsei University, Seoul 120-749, Republic of Korea

ARTICLE INFO

Article history:
Received 2 May 2010
Received in revised form
22 July 2010
Accepted 25 July 2010
Available online 1 August 2010

Keywords:
Zeolite
Gismondine
Pressure
Compressibility

ABSTRACT

Compression behaviour of a potassium aluminogermanate with a gismondine framework topology (K-AlGe-GIS) was studied using in-situ high-pressure synchrotron X-ray powder diffraction. In contrast to the potassium gallosilicate analogue (K-GaSi-GIS), no elastic anomaly due to pressure-induced hydration and/or cation relocation was observed in K-AlGe-GIS. The Birch–Murnaghan fit to the pressure–volume data results in a bulk modulus of $B_0=31(1)$ GPa. The derived linear-axial compressibilities (i.e., $\beta_a=0.0065(5)$ GPa^{-1}, $\beta_b=0.0196(4)$ GPa^{-1}, $\beta_c=0.0081(7)$ GPa^{-1}) indicate that the *b*-axis, normal to the 8-ring channels, is about three times more compressible than the *a* and *c* axes, parallel to the elliptical 8-ring channels. As a consequence a gradual flattening of the so-called 'double crankshaft' structural building units of the gismondine framework is observed. In K-AlGe-GIS, this flattening occurs almost linear with pressure, whereas it is nonlinear in the GaSi-analogue due to structural changes of the water–cation assembly under hydrostatic pressures.

1. Introduction

Structural investigations of zeolites under hydrostatic pressure have revealed unusual changes in the host–guest chemistry as well as allowed a better understanding of their basic elastic behaviour under pressure [1–7]. One of the distinctive features that zeolites exhibit under hydrostatic pressure is the possibility of insertion of molecules such as water or small gas molecules and cations from the surrounding pressure-transmitting medium into the zeolitic pores/channels. In such cases, the elastic behaviour of zeolites deviates from depending in a linear fashion on pressure and exhibits non-linearities and/or discontinuities of their compressibilities [4,8]. Amongst other factors the flexibility of the zeolitic framework along with the non-framework cation and/or molecular assemblies within the pores and channels plays an important role in the high pressure chemistry of zeolites. The gismondine framework has been known to be one of the most flexible among the 191 known topologies [9]. Recently we have shown that the synthetic potassium gallosilicate with a gismondine topology exhibits modulation discontinuity in its compressibility due to pressure-induced hydration and a subsequent order–disorder-type rearrangement of the cation–water assembly under pressure [10].

The framework of a GIS-type zeolite is composed of two double 'crankshaft' chains of tetrahedrons that are connected perpendicular to each other (Fig. 1) [11–13]. The resulting three-dimensional framework possesses interconnected pores and channels that are accessed through 8-ring openings. In the mineral gismondine (ideally, $Ca_4Al_8Si_8O_{32}\cdot 16H_2O$) the silicon and aluminium cations are in the centre of oxygen tetrahedrons which are either ordered or disordered depending on the Si/Al ratio: they are ordered when the ratio is close to unity [13,14] and disordered when Si-rich [15,16]. Other members of this structural family with GIS-type frameworks containing Be-, P-, Ga-, and GeO_4 tetrahedra have also been reported [17–20]. There are many different exchangeable non-framework cations which control the zeolitic water content and other physical properties [21,22]. The varied framework chemistry coupled with the easy ion-exchange properties is a sign that the GIS-type framework is quite adaptable. In fact, numerous structural studies on GIS-type zeolites have been reported as a function of cation substitution and temperature-induced dehydration. These studies reveal the largest range of unit cell variations and symmetries thus far encountered in a single framework-type zeolite [21,23,24]. Recently the structural effect of hydrostatic pressure on the gismondine-type framework and its cation–water sublattice has been reported for the mineral aluminosilicate gismondine [25]

* Corresponding author. Fax: +82 2 392 6527.
E-mail address: yongjaelee@yonsei.ac.kr (Y. Lee).

0022-4596/$ - see front matter © 2010 Elsevier Inc. All rights reserved.
doi:10.1016/j.jssc.2010.07.041

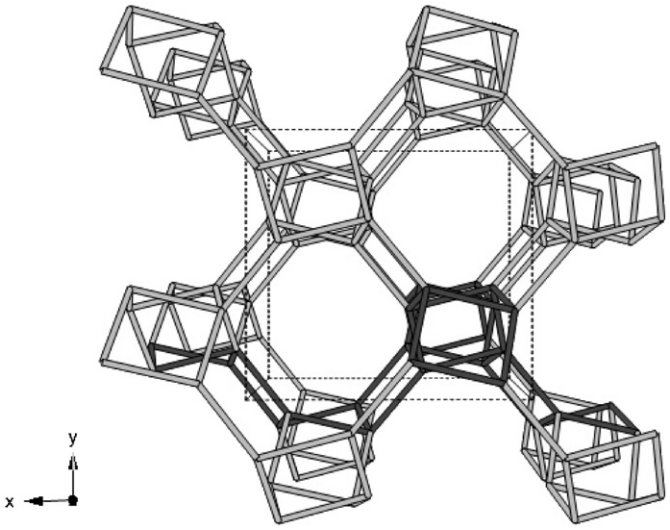

Fig. 1. A stick representation of the gismondine-type aluminogermanate framework structure viewed perspective along the [010]. The cross-linking of the two double crankshaft chain units is emphasized with dark grey. Vertices correspond to T (Al and Ge in alternation) atoms. Framework oxygen atoms and extra framework species are omitted for clarity. Dotted lines outline a unit cell.

and a synthetic gallosilicate analogue [10]. In order to understand the influence of different framework compositions on the high pressure chemistry we have investigated a synthetic aluminogermanate gismondine and report here on the comparative elastic behaviour of the gismondine framework under pressure based on in-situ high-pressure synchrotron X-ray powder diffraction data.

2. Experimental methods

The synthesis of K-AlGe-GIS was described in detail by Tripathi et al. [19]. Initial characterization and screening to find suitable experimental conditions were performed using a symmetric diamond-anvil cell and an imaging plate detector at 5A-HFMS beamline at Pohang Accelerator Laboratory (PAL). *In situ* high-pressure synchrotron X-ray powder diffraction experiments were performed at the X14A beamline at the National Synchrotron Light Source (NSLS) at Brookhaven National Laboratory (BNL). The primary white beam from the bending magnet was monochromatized using a Si (111) crystal, and sets of parallel slits were used to create a ~400 μm beam of monochromatic X-rays with a wavelength of 0.6474 Å. A Si-strip detector prototype consisting of a monolithic array of 640 silicon diodes coupled to a set of BNL's HERMES application-specific integrated circuits (D.P. Siddons, Private communications) was used to collect powder diffraction data ($\Delta d/d \sim 10^{-3}$). The Si-strip detector covered 3.2° in 2θ and was stepped in 2° intervals over the angular range 3.5–35.5° with counting times of 30 s per step. The wavelength of the incident beam was determined using a LaB_6 standard (SRM 660).

A modified Merrill–Bassett diamond anvil cell (DAC) was used for the high-pressure experiments, equipped with two type-I diamond anvils (culet diameter of 800 μm) and tungsten-carbide supports [26]. A stainless-steel foil of 250 μm thickness was pre-indented to a thickness of about 100 μm, and a 500 μm hole was obtained by electro-spark erosion. The powdered sample of K-AlGe-GIS was placed in the gasket hole together with some ruby chips for in-situ pressure measurements. Ambient pressure data were collected on the dry powder sample inside the DAC. Subsequently, a methanol:ethanol:water (16:3:1 by volume) mixture was added to the sample chamber as a hydrostatic pressure-transmitting medium, and then the DAC was sealed to the first pressure point. The pressure the sample was exposed to in the DAC was measured by detecting the shift in the R1 emission line of included ruby chips (precision: ±0.05 GPa) [27]. The sample was typically equilibrated for about 10 min in the DAC at each measured pressure. After each powder diffraction pattern was collected, the pressure was increased in increments of ~0.5 GPa. A selected region of the synchrotron X-ray powder diffraction pattern at each measured pressure is shown in Fig. 2.

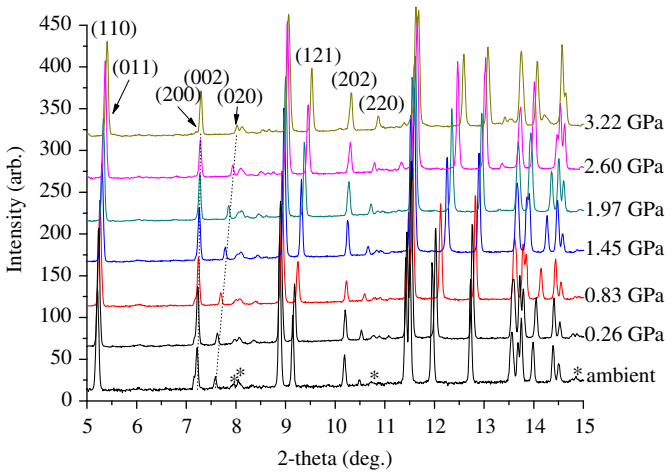

Fig. 2. Details of the changes in the synchrotron X-ray powder diffraction patterns observed for K-AlGe-GIS as a function of hydrostatic pressure mediated by alcohol and water mixture. Dotted lines are guides to the eyes to show anisotropic shifts in Bragg peak positions. Asterisk marks indicate peaks from impurity.

Table 1
Changes in the unit cell lengths and volume of K-AlGe-GIS as a function of applied hydrostatic pressure mediated by alcohol and water mixture at room temperature.

K-AlGe-GIS[a] (GPa)	a (Å)	b (Å)	c (Å)	β (deg.)	V (Å^3)
Ambient	10.3206(3)	9.7533(2)	10.2376(3)	90.107(2)	1030.51(7)
0.26	10.3035(2)	9.6989(2)	10.2176(2)	90.100(1)	1021.07(4)
0.83	10.2744(2)	9.5983(2)	10.1920(2)	90.034(1)	1005.10(5)
1.45	10.2441(2)	9.4942(2)	10.1711(2)	90.101(2)	989.23(5)
1.97	10.2303(2)	9.4191(2)	10.1642(2)	89.821(1)	979.42(6)
2.60	10.2127(3)	9.3265(2)	10.1525(3)	90.208(2)	967.00(6)
3.22	10.1888(3)	9.2313(2)	10.1341(3)	90.227(1)	953.16(7)

[a] Space group $I2/a$ was used throughout.

The whole profile fitting was performed using the GSAS suite of programs [28]. The background was fitted by a linear interpolation between selected positions in 2θ, and the pseudo-Voigt profile function proposed by Thompson et al. was used to model the observed Bragg peaks [29]. Attempts to perform full-matrix Rietveld analysis were not successful due to the insufficient powder averaging effects. The final refined unit cell parameters from the ambient to 3.22 GPa data are listed in Table 1.

3. Results and discussion

An anisotropic compression behaviour can be deduced by inspecting the powder diffraction pattern (Fig. 2), which reveals that the shifts of the peaks in 2θ with increasing pressure are not monotonic and dependent on the Miller indices (hkl). For example, (020) peak shifts farther to higher 2θ on pressure

increase than (200) and (002) peaks do. The evolution of the monoclinic unit cell lengths of K-AlGe-GIS, derived from a series of full profile fitting procedure as described above, clearly indicates anisotropic contraction behaviour (Fig. 3a), resulting in a gradual and continuous unit cell volume contraction (Fig. 3b). This contrasts the changes observed in K-GaSi-GIS, which showed two distinct regions of volume contraction separated by an initial pressure-induced hydration and subsequent order–disorder transition at higher pressures [10]. Therefore, we suspect that the observed changes in the elastic parameters of K-AlGe-GIS would reflect isochemical and isostructural compression. The volume compressibility of K-AlGe-GIS was determined using the Birch–Murnaghan Equation of State (BM-EoS), which is based upon the assumption that the high-pressure strain of a solid can be expressed as a Taylor series of the Eulerian strain [30]

$$f = [(V_0/V)^{2/3} - 1]/2$$

(V_0 and V represent the unit-cell volume, under ambient and high-pressure conditions, respectively). Expansion in the Eulerian strain yields the following isothermal Equation-of-State:

$$P(f) = 3K_0 f(1+2f)^{5/2}\{1 + 3/2(K'-4)f + 3/2[K_0K'' + (K'-4)(K'-3) + 35/9]f^2 + \cdots\}$$

where K_0 represents the bulk modulus, defined as $K_0 = -V_0(\partial P/\partial V)_{P=0} = 1/\beta$; where β is the volume compressibility coefficient, and K' and K'' represent the first and second derivatives of the bulk modulus with respect to pressure ($K' = \partial K_0/\partial P$; $K'' = \partial^2 K_0/\partial P^2$). The derived bulk modulus of K-AlGe-GIS is 31(1) GPa with K' of 8(1). This value constitutes one of the smallest intrinsic bulk moduli in zeolites measured thus far [31]. Furthermore, in comparison to K-GaSi-GIS, this value is by ca. 55% smaller than the one observed in the low pressure phase I (K_0=69(1) GPa) and by 24% smaller than the one measured in the high pressure phase II (K_0=41(2) GPa). This is again indicative of the absence of any major chemical or structural changes in K-AlGe-GIS under pressure.

The anisotropic elastic behaviour of the unit cell axes lengths can be described quantitatively with a "linearized" BM-EoS, substituting the cube of lattice parameter with the volume [30]. The "linear-K_0", or "axial-K_0", obtained is related to the linear–axial compressibility coefficient (β_j) by

$$\beta_j = -1/(3K_{0j}) = (1/l_{0j})(\partial l_j/\partial P)$$

where l_{0j} ($j = a, b, c$) is the length of the unit cell axis length under room conditions. The derived linear-axial compressibilities are β_a=0.0065(5) GPa^{-1}, β_b=0.0196(4) GPa^{-1}, β_c=0.0081(7) GPa^{-1}. The elastic anisotropy of K-AlGe-GIS is thus pronounced along the b-axis, being β_a:β_b:β_c=1.0:3.0:1.2. This anisotropy might be explained by the framework topology. Being close to tetragonal symmetry [9], the monoclinic unit cell of K-AlGe-GIS is a result of the cross linking of the dense double 'crankshaft' chains along the a- and c-axes. Compression along these two axes would induce further buckling of the double 'crankshaft' chains and thus results in an energetically less favourable structure toward framework collapse. On the other hand, the b-axis is normal to the cross-linked double 'crankshaft' chains, and compression along this axis would lead to a compaction of the elliptical 8-ring channels by flattening the double 'crankshaft' chains. This can be rationalized as the pressure-induced evolution of the planarity (or linearity) of the double 'crankshaft' chains (Fig. 4). The planarity of the double 'crankshaft' chains can be defined by one full unit length of the chain, i.e., the a- or c-axis length, divided by its height, i.e., half of the b-axis length (Fig. 1). In K-AlGe-GIS, both chains show a linear monotonic increase of the planarity under pressure. In K-GaSi-GIS, on the other hand, the pressure-induced evolution of the planarity of the chain is non-linear and exhibits different regions of increase due to chemical and structural changes occurring under pressure (Fig. 4).

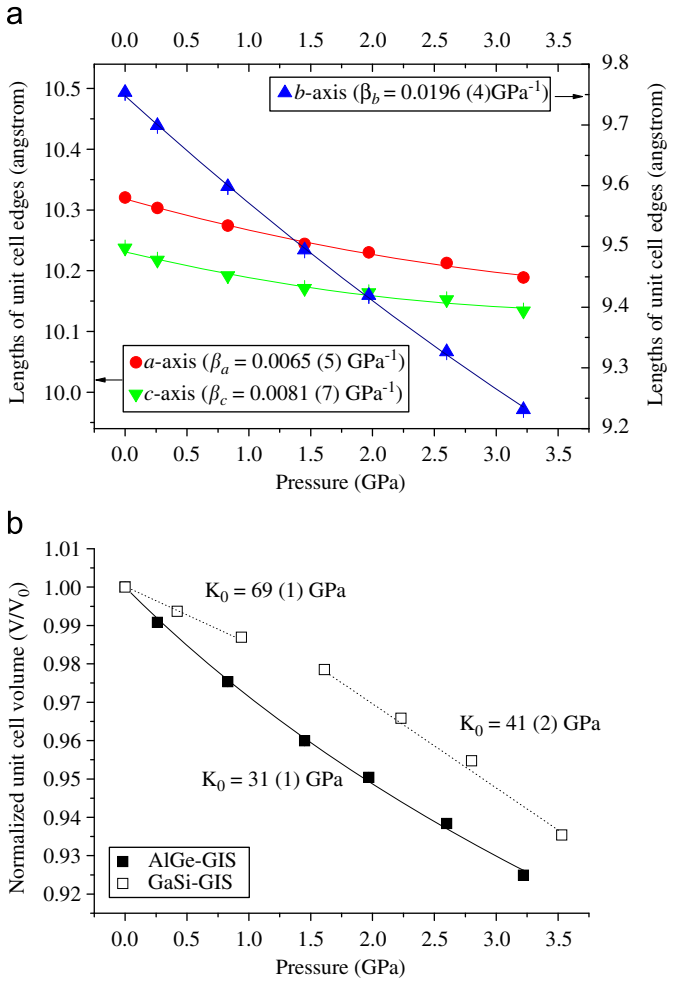

Fig. 3. Changes in (a) the unit cell edge lengths and (b) volume of K-AlGe-GIS as a function of the applied hydrostatic pressures. Data from K-GaSi-GIS are shown as open symbols for comparison.

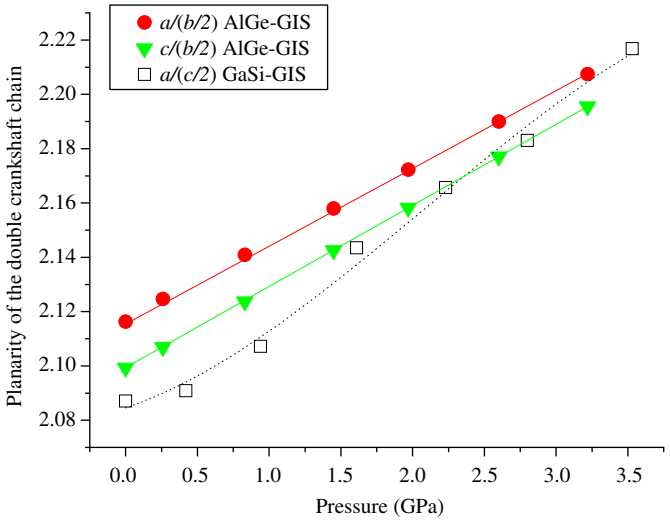

Fig. 4. The pressure-induced evolution of the planarity of the double crankshaft chain defined by the one full unit length of the chain, i.e., the a- or c-axes length, divided by its height, i.e., half of the b-axis length. Data from K-GaSi-GIS are shown as open symbols for comparison.

The absence of pressure-induced structural changes in the channels of K-AlGe-GIS, compared to K-GaSi-GIS, cannot be assessed without detailed atomistic models from Rietveld analysis. In terms of the packing in the channels at ambient conditions, both compounds show similar cation–water contents based on their unit cell formulae, i.e., ca. $4K^+$–$4H_2O$ per channel in K-AlGe-GIS and ca. $2.9K^+$–$5H_2O$ per channel in K-GaSi-GIS [19,20]. The flexibility of the AlGe- and GaSi-frameworks also appears not to be drastically different based on changes in the elastic parameters under pressure. The differences in the degree of ordering and binding energy of the non-framework cations and water molecules might be important to induce further hydration under pressure and subsequent rearrangement of the non-framework species within the compressed channels. Efforts to increase both the accuracy and precision in the high pressure experiment will clarify the different host–guest chemistry of the gismondine zeolites under pressure.

4. Conclusion

We have investigated the high pressure elastic behaviour of a synthetic potassium aluminogermanate with a gismondine framework structure and observed the oriented unit cell contraction due to the flattening of the double "crankshaft" chain units. Compared to the previously investigated pressure-induced hydration and order–disorder transition observed in a gallosilicate analogue, hydrostatic pressure mediated by alcohol and water mixture does not seem to cause any apparent structural changes of the framework or chemical exchange within the channels of K-AlGe-GIS. The derived bulk modulus of K-AlGe-GIS represents the inherent compressibility of the AlGe-gismondine framework and qualifies K-AlGe-GIS as one of the softest zeolites reported thus far. We thus demonstrated the similarities and differences of the high-pressure chemistry between different chemical analogues with the gismondine structure. Pressure-induced insertion of other smaller atoms or molecules into the non-penetrating K-AlGe-GIS channel might be envisaged for future high pressure applications.

Acknowledgments

This work was supported by the Utilization and Sequestration of CO_2 using Industrial Minerals program by KIGAM. TV, CCK, and YL also thank the support by the Global Research Lab Program of the Ministry of Education, Science and Technology (MEST) of the Korean Government. Experiments at PAL were supported in part by MEST and Pohang University of Science and Technology (POSTECH). Research carried out in part at the NSLS at BNL is supported by the U.S. Department of Energy, Office of Basic Energy Sciences. The authors thank the use of Ruby laser system at NSLS which was supported by COMPRES, the Consortium for Materials Properties Research in Earth Sciences, under NSF Cooperative Agreement EAR 06-49658.

References

[1] I.A. Belitsky, B.A. Fursenko, S.P. Gubada, O.V. Kholdeev, Y.V. Seryotkin, Phys. Chem. Mineral. 18 (1992) 497–505.
[2] G.D. Gatta, Eur. J. Mineral. 17 (2005) 411–421.
[3] J.N. Grima, R. Gatt, V. Zammit, J.J. Williams, K.E. Evans, A. Alderson, R.I. Walton, J. Appl. Phys. 101 (2007) 086102.
[4] R.M. Hazen, Science 219 (1983) 1065–1067.
[5] Y. Lee, T. Vogt, J.A. Hriljac, J.B. Parise, G. Artioli, J. Am. Chem. Soc. 124 (2002) 5466–5475.
[6] Y. Lee, T. Vogt, J.A. Hriljac, J.B. Parise, J.C. Hanson, S.J. Kim, Nature 420 (2002) 485–489.
[7] P.F. McMillan, Nat. Mater. 1 (2002) 19–25.
[8] Y. Lee, J.A. Hriljac, J.B. Parise, T. Vogt, Am. Mineral. 90 (2005) 252–257.
[9] C. Baerlocher, L.B. McCusker, D.H. Olson, in: Atlas of Zeolite Framework Types, sixth ed, Elsevier, Amsterdam, 2007.
[10] Y. Lee, S.K. Kim, C.C. Kao, T. Vogt, J. Am. Chem. Soc. 130 (2008) 2842–2850.
[11] C. Baerloch, W.M. Meier, Z. Kristallogr. 135 (1972) 339.
[12] D.W. Breck, N.A. Acara, US Patent 711 (1968) 565.
[13] K. Fischer, Am. Mineral. 48 (1963) 664–672.
[14] A. Alberti, G. Vezzalini, Acta Crystallogr. 35 (1979) 2866–2869.
[15] G. Artioli, Am. Mineral. 77 (1992) 189–196.
[16] L.B. McCusker, C. Baerlocher, R. Nawaz, Z. Kristallogr. 171 (1985) 281–289.
[17] P. Feng, X. Bu, G.D. Stucky, Nature 388 (1997) 735–741.
[18] G.M. Johnson, A. Tripathi, J.B. Parise, Chem. Mater. 11 (1999) 10–12.
[19] A. Tripathi, J.B. Parise, S.J. Kim, Y. Lee, G.M. Johnson, Y.S. Uh, Chem. Mater. 12 (2000) 3760–3769.
[20] A. Tripathi, J.B. Parise, S.J. Kim, Y.J. Lee, Y.S. Uh, Acta Crystallogr. C 57 (2001) 344–346.
[21] T. Bauer, W.H. Baur, Eur. J. Mineral. 10 (1998) 133–147.
[22] A. Dyer, B. Heywood, N. Szyrokyj, Micropor. Mesopor. Mater. 92 (2006) 161–164.
[23] A.J. Celestian, J.B. Parise, C. Goodell, A. Tripathi, J. Hanson, Chem. Mater. 16 (2004) 2244–2254.
[24] G. Vezzalini, S. Quartieri, A. Alberti, Zeolites 13 (1993) 34–42.
[25] C. Betti, E. Fois, E. Mazzucato, C. Medici, S. Quartieri, G. Tabacchi, G. Vezzalini, V. Dmitriev, Micropor. Mesopor. Mater. 103 (2007) 190–209.
[26] H.K. Mao, R.J. Hemley, Philos. Trans. R. Soc. London A 354 (1996) 1315–1333.
[27] P.M. Bell, H.K. Mao, Carnegie Inst. Washington Year Book, 1979, pp. 665–669.
[28] B.H. Toby, J. Appl. Crystallogr. 34 (2001) 210–213.
[29] P. Thompson, D.E. Cox, J.B. Hastings, J. Appl. Crystallogr. 20 (1987) 79–83.
[30] R.J. Angel, in: R.M. Hazen, R.T. Downs (Eds.), Reviews in Mineralogy and Geochemistry: High-Temperature and High-Pressure Crystal Chemistry, The Mineralogical Society of America, Washington, DC, 2000, pp. 35–58.
[31] G.D. Gatta, Z. Kristallogr. 223 (2008) 160–170.